This paper is available on line at http://www.mcponline.org

Probing the Efficiency of Proteolytic Events by Positional Proteomics*[S]

Kim Plasman‡§†, Petra Van Damme‡§†‖, Dion Kaiserman¶, Francis Impens‡§, Kimberly Demeyer‡§, Kenny Helsens‡§, Marc Goethals‡§, Phillip I. Bird¶, Joël Vandekerckhove‡§, and Kris Gevaert‡§‖

Several mass spectrometry-driven techniques allow to map the substrate repertoires and specificities of proteases. These techniques typically yield long lists of protease substrates and processed sites with (potential) physiological relevance, but in order to understand the primary function of a protease, it is important to discern bystander substrates from critical substrates. Because the former are generally processed with lower efficiency, data on the actual substrate cleavage efficiency could assist in categorizing protease substrates. In this study, quantitative mass spectrometry following metabolic proteome labeling (SILAC), combined with the isolation of N-terminal peptides by Combined Fractional Diagonal Chromatography, was used to monitor fluxes in the concentration of protease-generated neo-N-termini. In our experimental setup, a Jurkat cell lysate was treated with the human serine protease granzyme B (hGrB) for three different incubation periods. The extensive list of human granzyme B substrates previously catalogued by N-terminal Combined Fractional Diagonal Chromatography (1) was then used to assign 101 unique hGrB-specific neo-N-termini in 86 proteins. In this way, we were able to define several sites as getting efficiently cleaved *in vitro* and consequently recognize potential physiologically more relevant substrates. Among them the well-known hGrB substrate Bid was confirmed as being an efficient hGrB substrate next to several other potential regulators of hGrB induced apoptosis such as Bnip2 and Akap-8. Several of our proteomics results were further confirmed by substrate immunoblotting and by using peptide substrates incubated with human granzyme B. ***Molecular & Cellular Proteomics 10: 10.1074/mcp.M110.003301, 1–10, 2011.***

Proteolysis is a process during which a target protein is either partially processed into (stable) fragments (often implicated in protease-mediated propagation of signaling events) or completely shred into its composite amino acids (protein catabolism) by proteolytic enzymes or proteases. Proteases have key effector roles in human homeostasis, pathogenesis, and autoimmunity, so not surprisingly, it is considered of utmost importance to elucidate their specific functions in these processes, among others by profiling their physiological substrate repertoires (2, 3). Because proteolytic cleavage results in the formation of new protein N- and C-termini, many efforts were recently devoted to the specific isolation of neo-terminal peptides. This resulted in the development of several proteomics technologies to study protease substrate specificities or catalogue substrate repertoires (*e.g.* recently reviewed in (4)).

Because of this highly evolving field of targeted proteomics, a wealth of protease-specific substrate cleavage data has emerged, which typically originate from *ex vivo* analyses; *e.g.* the hundreds of potential granzyme B substrates that were reported by our group (1). Several studies already indicated that the high sensitivity of mass spectrometers might also lead to the identification of very rare and inefficient cleavage events (*e.g.* (1, 5)). These are often believed to occur as the result of nonphysiological conditions of protease concentration and substrate localization (especially in *ex vivo* studies) and therefore affect proteins that are probably not of crucial importance to understand the physiological function of a protease. It has therefore become highly important to distinguish the key targets of proteases identified in such screens in order to reveal the primary signaling pathways or protein assemblies on which proteases act. Because it was also shown that substrate processing resulting in loss-of-function happens faster than processing resulting in gain-of-function (6), clear challenges to distinguish efficient from inefficient, and early from late substrate processing events in large-scale protease studies are emerging.

To discern bystander from critical cleavage events of human granzyme B (hGrB)[1]—a protease involved in granule-mediated cell death by cells from the innate and adaptive

From the ‡Department of Medical Protein Research, VIB, B-9000 Ghent, Belgium; §Department of Biochemistry, Ghent University, B-9000 Ghent, Belgium; ¶Department of Biochemistry and Molecular Biology, Monash University, Victoria 3800, Australia

Received July 16, 2010, and in revised form, October 29, 2010

Published, MCP Papers in Press, November 3, 2010, DOI 10.1074/mcp.M110.003301

[1] The abbreviations used are: (h)GrB, (human) granzyme B; (h)Bid, (human) BH3-interacting domain death agonist; AcD3, trideuteroacetyl; Akap-8, A-kinase anchor protein 8; Bnip2, BCL2/adenovirus E1B 19 kDa protein-interacting protein 2; COFRADIC, combined fractional diagonal chromatography; SILAC, stable isotope labeling by amino acids in cell culture; SRM, selected reaction monitoring.

immune system—we here used a three-plexed (time-based) N-terminal Combined Fractional Diagonal Chromatography (COFRADIC) positional proteomics setup. N-terminal COFRADIC uses consecutive reverse phase high performance liquid chromatography (RP-HPLC) separations of peptide mixtures and sorts out N-terminal peptides from whole proteome digests (7, 8). Metabolic proteome labeling was introduced by isotope variants of arginine because sorted N-terminal peptides, by nature of the used chemical modification reactions, all end on arginine. Here, three-plexed proteomics was performed using $^{12}C_6$, $^{13}C_6$, and $^{13}C_6{}^{15}N_4$ arginine stable isotope labeling by amino acids in cell culture (SILAC) labeling (9), introducing labels that provide ample spacing and thus allow direct quantification of the individual peptide ions (see Results section). Our general assumption was the following. For each identified protein N-terminal peptide and hGrB-generated neo-N-terminal peptide, three possible isotopic variants may be expected. Protein N termini that are not affected by hGrB and of which the concentration remains constant, can be easily read from their MS spectra. On the other hand, in our time-based proteomics setup, different trends for neo-N-termini generated by hGrB are expected. We show that hGrB cleavage sites fully cleaved at the shortest time of incubation—and as such assigned as efficient cleavage sites—are readily distinguished from less efficient sites based on the pattern of their isotopically labeled peptide ions in MS spectra. Validation of the cleavage efficiency of several categorized hGrB sites was done by immunoblot detection following SDS-PAGE separation, in addition to monitoring *in vitro* peptide processing by RP-HPLC. Furthermore, kinetics of processing was analyzed for several representative substrates. The results of all these biochemical characterization experiments were very well in agreement with the data obtained from the proteomics screen, among others confirming the known human BH3-interacting domain death agonist as a crucial and efficiently cleaved hGrB substrate, thus validating our targeted proteomics approach for identifying prime targets of proteases.

EXPERIMENTAL PROCEDURES

Cell Culture—Human Jurkat T cells were from the ATCC (TIB-152, American Type Culture Collection, Manassas, VA) and were grown in RPMI 1640 medium supplemented with 10% dialyzed fetal bovine serum (Invitrogen, Carlsbad, CA), 100 units/ml penicillin (Invitrogen), and 100 μg/ml streptomycin (Invitrogen). Cells were grown in media containing either natural ($^{12}C_6$), $^{13}C_6$, or $^{13}C_6{}^{15}N_4$ L-arginine (Cambridge Isotope Labs, Andover, MA) (9) at a concentration of 230 μM (*i.e.* 20% of the suggested concentration present in RPMI at which L-arginine to proline conversion was not detectable). Cells were cultured at 37 °C and in 5% CO_2 for at least six population doublings to ensure complete incorporation of the labeled arginine.

Preparation of Cell Lysates for N-Terminal COFRADIC Analysis—SILAC-labeled cells were washed in D-PBS and resuspended at 7×10^6 cells per ml in 50 mM Tris-HCl and 100 mM NaCl at pH 8.0. Cells were pre-incubated with the pan-caspase inhibitor N-benzyloxycarbonyl-Val-Ala-Asp-fluoromethyl ketone at a final concentration of 50 μM for 15 min at 37 °C and then lysed by three rounds of freeze-thawing. Supernatants, cleared by centrifugation for 10 min at 16,000 $\times$ *g* (the protein concentration was determined to be 1.3 mg/ml), were treated with 200 nM of human recombinant granzyme B (hGrB) for different time-points at 37 °C. Recombinant human granzyme B was expressed and purified from *Pichia pastoris*, and its activity was determined as described previously (10, 11). Solid guanidinium hydrochloride was added to a final concentration of 4 M in order to inactivate hGrB and denature all proteins. Before mixing the samples in equal amounts, proteins were reduced and alkylated simultaneously, using tris(2-carboxyethyl)phosphine.hydrochloride (TCEP.HCl; 1 mM final concentration) and iodoacetamide (2 mM final concentration) respectively, for 1 h at 30 °C. Subsequent steps of the N-terminal COFRADIC protocol were performed as described previously (7). The proteome was digested overnight at 37 °C with sequencing-grade, modified trypsin (Promega, Madison, WI) (enzyme/substrate of 1/100 w/w).

Liquid Chromatography (LC)-tandem MS (MS/MS) Analysis and Data Processing—Electrospray ionization (ESI) LC-MS/MS analysis was performed on an ESI-quadrupole (Q)-time-of-flight (TOF) (Waters Corporation) mass spectrometer as described before (12). ESI-Q-TOF MS/MS peptide fragmentation spectra were converted to pkl files using the Masslynx® software (version 4.1, Waters Corporation). N-terminal peptides were identified using a locally installed version of the MASCOT database search engine version 2.2.1 (www.matrixscience.com) and the Swiss-Prot database (version 57.11 of UniProtKB/Swiss-Prot protein database, containing 512,994 sequence entries of which 20,328 originated from human) was searched with restriction to human proteins. Truncated peptide databases made by DBToolkit (13), were searched in parallel to pick up protein processing events more efficiently (*e.g.* (14)). The following search parameters were used. Peptide mass tolerance was set at 0.2 Da and peptide fragment mass tolerance at 0.1 Da with the ESI-QUAD-TOF as selected instrument for peptide fragmentation rules for the Q-TOF Premier data. Endoproteinase Arg-C/P (= no restriction towards arginine-proline cleavage) was set as enzyme allowing one missed cleavage. Variable modifications were pyroglutamate formation of N-terminal glutamine, pyrocarbamidomethyl formation of N-terminal alkylated cysteine, deamidation of asparagine, acetylation and trideuteroacetylation of the alpha-N-terminus. Fixed modifications were methionine oxidation (sulfoxide), carbamidomethyl for cysteine, trideuteroacetylation of lysine and for identifying heavy labeled peptides, [$^{13}C_6$] or [$^{13}C_6{}^{15}N_4$]-arginine were additionally set as fixed modifications. Only MS/MS-spectra and corresponding identifications that exceeded the corresponding MASCOT's threshold score of identity (at 95% confidence level) and that were ranked one, were withheld. In addition, spectra that received a low MASCOT ion score (five or less points above threshold for identity) were further interrogated and only spectra that contained b- and y-fragment ions covering a stretch of three consecutive amino acids were considered identified (see Supplemental Data listing identified MS/MS-spectra). The estimated false discovery rate by searching decoy databases was typically found to lie between 2% and 4% on the spectrum level (7). Whenever a peptide matched to multiple members of a protein family (redundancy), the protein entry reported (column "Protein description," Supplemental Table 1) was according to its alphabetical ranking. In each case, other matching protein entries were reported under the column "Isoforms." Corresponding orthologous mouse cleavage sites, as determined in (1), are reported in Supplemental Table 1.

The peptide intensity ratios were individually calculated from the MS data in the Masslynx® software version 4.1 environment. In order to correct for small variations in initial protein concentrations, the $^{12}C_6/^{13}C_6$ and $^{12}C_6/^{13}C_6{}^{15}N_4$ ratios of the 1788 database-annotated protein N-terminal peptides (peptides starting at position 1 or 2) were first subjected to robust statistics using base-2 logarithm values of

their ratios (15). The corresponding ratio means, being 0.0115 ($^{12}C_6/^{13}C_6$) and −0.0209 ($^{12}C_6/^{13}C_6{}^{15}N_4$), were then used to correct for the calculated ratios of all peptides identified. Then, we used the R software package for statistical computing to calculate the probability distributions of log2 transformed N-terminal peptide ratios between the first and second time point (*N*(0.0115, 0.1416) (mean, standard deviation)) and between the second and third time point (*N*(-0.0209, 0.1890)). Protease substrate intensity ratios falling within the 99.5% probability interval of the protein N-terminal peptide intensity ratios were considered as derived from efficient cleavage sites (see Results section).

Immunoblot Analysis—To inactivate endogenous caspases, and thus exclude caspase-mediated cleavage of tested substrates following granzyme B activation, all protein samples, except for a control sample and a sample incubated with 100 nM hGrB for 2 h (the latter samples demonstrate that the GrB-activity potential was unaltered when making use of alkylated protein lysates), were pretreated with iodoacetamide for 15 min in the dark at a final concentration of 5 mM (16, 17). Subsequently, all protein samples were prepared and treated with hGrB at different concentrations and for different time-points (see Results section). Following hGrB incubation, sample loading buffer was added and equal amounts of protein (50 μg/sample; protein concentrations were measured using the DC Protein Assay Kit from Bio-Rad (Munich, Germany)) were separated on 4%–12% or 12% polyacrylamide Criterion XT-gels in MOPS buffer (Bio-Rad) at 150 V. Subsequently, proteins were transferred onto a PVDF-membrane. Membranes were blocked for 30 min in 5% skimmed milk powder containing Tris-buffered saline and 0.1% Tween-20 (TBS-T) and probed for 1 h with primary antibody in 5% skimmed milk powder in TBS-T. Following three 10 min washes in TBS-T, membranes were incubated with species-specific HRP-conjugated antibody for 1 h in 5% skimmed milk powder containing TBS-T. Again following a three-fold wash in TBS-T or TBS (last wash step), bands were visualized on ECL Hyperfilms (Amersham Biosciences, Buckinghamshire, UK) using an enhanced chemiluminiscence kit (PerkinElmer Life Sciences, Boston, MA). The caspase-3 antibody was from Calbiochem (AAP-113), Bid-antibody from R&D systems (AF860) (Minneapolis, MN), nucleolin antibody from Abcam (ab16940) (Cambridge, MA), Akap-8 and importin α-4 antibody from Abcam (ab32822 and ab6038). Recombinant glutathione S-transferase (GST)-tagged Bnip2 was from Abnova (H00000663-P01) (Taipei, Taiwan) and was assayed with a GST antibody from Abcam (ab6649). The degree of processing was determined by densitometry following Western blot analysis of various substrates that were processed with various concentrations of human GrB and following various time-points of incubation. Quantification was performed using the ChemiGenius imaging system (SynGene, Cambridge, UK) and signal intensity was quantified using GeneTools 3.07 image analysis software (SynGene).

Confirmation of hGrB-Specific Cleavage Events by Treating Synthesized Peptides with hGrB—The following peptides holding hGrB cleavage sites were synthesized in-house using the Fmoc-chemistry on an Applied Biosystems 433A Peptide Synthesizer: NH_2.RLGRIEADSESQEDIIRY$_{(NO2)}$R.OH (Bid), NH_2.LPEDDSIEADILAITGY$_{(NO2)}$R.OH (Bnip2), NH_2.KETPEEVAADVLAEVIY$_{(NO2)}$R.OH (Akap-8), NH_2.VPHEDICEDSDIDGDY$_{(NO2)}$R.OH (importin α-4), and NH_2.FVKGLSEDTTEETLKY$_{(NO2)}$R.OH (nucleolin). Substrate peptides were assayed for 2 h at 37 °C with various hGrB concentrations (10, 50, 200, and 500 nM) at a substrate concentration of 100 μM. The reactions were stopped by adding trifluoroacetic acid to a final concentration of 1%. Cleavage by hGrB was assessed by monitoring the UV absorbance signal (214 nm) of the precursor peptide and its fragments by reverse phase-HPLC separation. The extent of hydrolysis was determined by comparing the intensity of the product peak(s) with that of the unprocessed precursor.

Analysis of the Granzyme B Cleavage Efficiency of the Fluorogenic Peptide Ac-IEPD-AMC in a Buffer and in a Cell Lysate—Ac-IEPD-AMC was purchased from Bachem (Bubendorf, Switzerland) and a 20 mM stock solution was prepared in DMSO. Freeze-thaw lysates of human Jurkat T-cells were made in a buffer containing 100 mM NaCl, 50 mM Tris-HCl pH 7.9 and these lysates were S-alkylated and desalted as described above. Measurements were performed in black 96-well plates on a temperature-controlled Bio-Tek FLx800 fluorescence microplate reader (excitation at 360 nm, emission at 460 nm). A 40 μl aliquot of a 400 nM granzyme B solution (150 mM NaCl, 50 mM Tris-HCl, pH 7.9) was added in every well while the plate was kept on ice. In a different plate, Ac-IEPD-AMC was diluted to twice the indicated final concentration in buffer or in the cell lysate (the protein concentration in the cell lysate was 2.6 mg/ml). A 40 μl aliquot of the hence diluted Ac-IEPD-AMC was then added to the wells containing granzyme B. The plate was briefly mixed and placed in the microplate reader at 37 °C. Over a period of 50 min, fluorescence was measured every 78 s.

RESULTS

General Description of the Proteomics Setup—Human Jurkat cells were grown in three different SILAC media containing $^{12}C_6$,$^{13}C_6$, or $^{13}C_6{}^{15}N_4$ L-arginine (Fig. 1*A*). Prior to freeze-thaw lysis, cells were treated with *N*-benzyloxycarbonyl-Val-Ala-Asp-fluoromethyl ketone to prevent substrate processing by caspases that are known to get activated by granzyme B (18). These different cell lysates were incubated with hGrB for 10, 30 or 60 min respectively (three-plex setup, Fig. 1*A*) and following protease inactivation, equal sample amounts were mixed and N-terminal peptides were isolated by the N-terminal COFRADIC sorting procedure (7). Subsequent LC-MS/MS analysis resulted in the identification of 2666 MS/MS-spectra that were linked to 992 peptides. Of these, 295 peptides (29.7%) present in 261 proteins were trideutero-acetylated, did not start at protein position one or two and thus formed our primary pool of potential hGrB recognized cleavage sites and substrates. This list was cross-checked with our previously reported catalogue of GrB processing events (1) and in this way, 101 unique neo-N-termini in 86 proteins (*i.e.* 34.2% of all neo-N termini identified in this study) were assigned as resulting from hGrB-mediated processing (Supplemental Table 1).

Our hypothesis was that efficient hGrB sites are cleaved to completeness at the shortest incubation time and thus the concentration of their corresponding neo-N-terminal peptides was not expected to increase upon prolonged hGrB incubation (Fig. 1*C*). Therefore, the MS pattern of these peptides was expected to resemble that of protein N-terminal peptides (Fig. 1*B*), whereas a less efficiently cleaved hGrB site should give rise to an increase of ion intensities in MS spectra at later time-points (Fig. 1*D*). Taking the intra-experimental ion signal variation of the protein N-termini into account, a category of efficiently cleaved hGrB sites was in this way identified within a 99.5% confidence interval. In fact, the averaged ratio values of 506 UniProt annotated protein N-terminal peptides (peptides with a protein start position of one or two) were calculated and used to delineate the most efficient hGrB cleavage sites (Fig. 2). The full list of hGrB-induced neo-N-termini, their ion intensity changes at the incubation times examined and

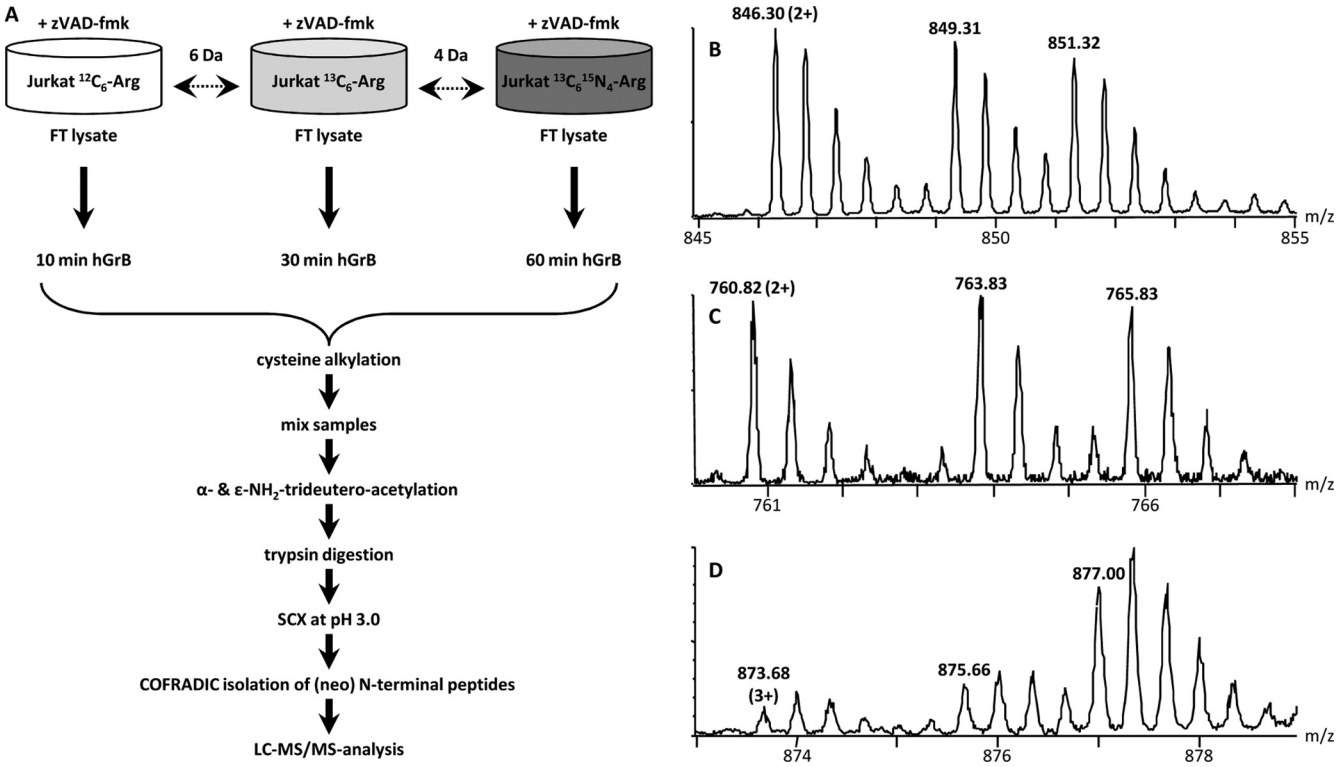

FIG. 1. **Experimental setup to probe the extent of substrate proteolysis by hGrB.** *A*, SILAC using $^{12}C_6$, $^{13}C_6$, and $^{13}C_6{}^{15}N_4$ L-arginine was used to label Jurkat cells and to then monitor concentration fluxes of (neo-)N-termini of zVAD-fmk pretreated Jurkat freeze-thaw (FT) cell lysates. $^{12}C_6$, $^{13}C_6$, and $^{13}C_6{}^{15}N_4$ L-arginine labeled lysates were *in vitro* incubated with 200 nM hGrB for respectively 10, 30, and 60 min. Following incubation and inactivation of hGrB by adding guanidinium hydrochloride, equal amounts of proteome preparations were mixed and N-terminal peptides were isolated by the N-terminal COFRADIC sorting procedure (7), the different key steps of which are indicated. *B*, A representative MS-spectrum showing the hGrB unaffected and thus unaltered N-terminus Ac-^{2}MLGPEGGEGFVVKLR^{16} (Ac denotes an α-acetylated amino group) from the heterogeneous nuclear ribonucleoprotein F (hnRNPF). *C*, A similar MS-profile was observed for an hGrB generated neo-N-terminus (AcD3-^{692}SGGNTSPGVTANGEAR^{707} (AcD3 denotes a trideutero-acetylated α-amino group)) from Rho/Rac guanine nucleotide exchange factor 2 (ARHG2), indicating an efficient cleavage event. *D*, Increasing ion intensities were observed for AcD3-^{484}SGLITPGGFSSVPAGMETPELIELR^{508} from the splicing factor 3B subunit 2 (SF3B2) hinting to a less efficiently cleaved hGrB site.

their assignment as efficient or less efficient sites is given in Table I. Besides the well-characterized and highly efficient hGrB substrate BH3-interacting domain death agonist or Bid, the pro-apoptotic Bcl-2 family member Bnip2, and the protein kinase A anchor protein 8 (Akap-8) were found to hold efficiently cleaved hGrB sites (fold changes observed between 10 and 30 min, and 30 and 60 min were 0.97 and 1, and 1.31, and 1.21 respectively). Of note is that all these proteins were previously reported to play prominent roles in the process of apoptotic execution under physiological conditions (19, 21, 27).

When searching for amino acid sequence biases between highly efficient and less efficiently cleaved sites, the inspection of P4 to P1 amino acid occurrences in cleavage sites categorized as efficient sites reveals a consensus recognition motif much alike the one deduced from positional scanning substrate combinatorial library data (22); IEPD (data not shown). In our study, an increased relative occurrence of proline at the substrate P2 position was observed for highly efficiently cleaved sites: 6 out of 18 of these preferred sites (33%) and only 9 out of 83 (10.8%) of the less preferred sites have Pro at P2. In addition, considering the relative occurrences of isoleucine, leucine and valine, these amino acids occupy P4 in 14 out of 18 (77.78%) preferred sites and only 42 out of 83 (50.6%) less preferred sites. Of further note is the fact that alternative P1 residue cleavages such as glutamate, as described in (1), were never categorized to efficiently cleaved sites (11 of the 83 less efficient sites harbored a glutamate at P1). Taken together however, these subtle differences indicate that at least for hGrB, experimental analysis as opposed to *in silico* prediction remains a prerequisite to assign the efficiency of cleavage.

Biochemical Characterization of Human Granzyme B Processing Efficiency by Substrate Immunoblot Analysis—To confirm our proteomics data, the efficiency of substrate cleavage was determined by applying densitometry following protein immunoblot analysis for Bid, Bnip2, Akap-8, importin α-4, and nucleolin. Substrate processing was assessed with various concentrations of hGrB and at various times of incubation. Immunoblot analysis of caspase-3 and its derived proteolytic fragments confirmed the activity of hGrB

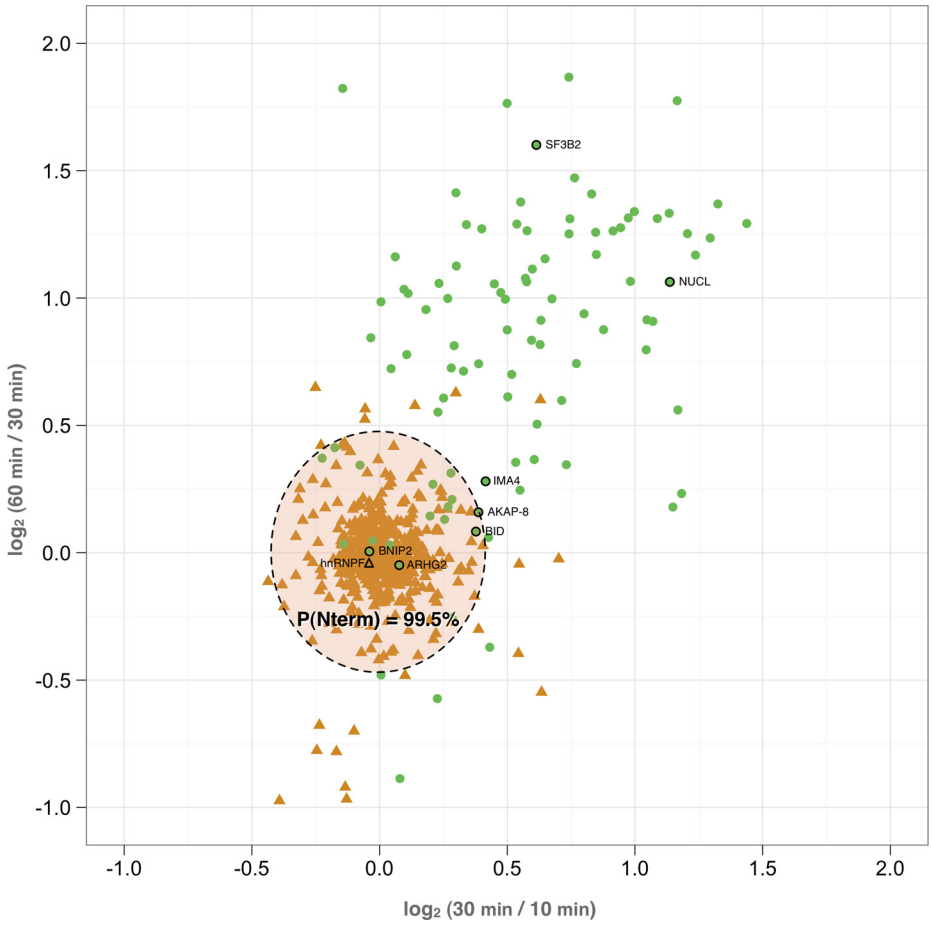

FIG. 2. **Classification of the most efficiently cleaved hGrB sites.** The distribution of 506 unique protein N-termini starting at position one or two (triangles) and 101 unique hGrB specific neo-N-termini (circles) of which the $^{13}C_6/^{12}C_6$ and $^{13}C_6{}^{15}N_4/^{13}C_6$ ratio could be calculated, is plotted. The spreading of ratio values for the unaffected protein N-termini was used to set the area containing the most efficiently cleaved hGrB sites ($p \geq 99.5\%$). Neo-N-termini or database annotated N-termini corresponding to the MS-spectra depicted in Fig. 1*B–D* and Fig. 3*A–E* are indicated.

on a natural substrate and showed iodoacetamide-mediated inhibition of downstream caspase activation by hGrB (Supplemental Fig. 1).

The MS-spectrum in Fig. 3*A* was assigned to the hGrB introduced neo-N-terminus ^{76}SESQEDIIR^{84} of Bid, representing an early, signal-inducing cleavage event and an established key substrate in the hGrB mediated apoptotic pathway (23). In accordance to the proteomics data where no further increase in ion signal intensity at later time-points was observed, immunoblotting of Bid revealed complete precursor cleavage at the earliest time point assayed at 200 nM of hGrB incubation. A similar MS-pattern in addition to an identical P4-P1 cleavage site recognition motif (IEAD^{28}) was observed for the neo-N-terminal peptide, ^{29}ILAITGPEDQPGSLEVNGNKVR^{50}, from Bnip2 (Fig. 3*B*). Immunoblotting of a 63 kDa N-terminal glutathione S-transferase (GST) tagged recombinant Bnip2 precursor protein showed the 30 kDa N-terminal fragment cleaved at IEAD^{28} as determined in the proteomics setup. Furthermore, densitometry confirmed Bnip2 as a highly efficient hGrB substrate as compared with Bid because the Bnip2 precursor was already cleaved for 95% following 2 h incubation with 10 nM of hGrB whereas Bid was cleaved for 76% under identical conditions (Fig. 4). The ion signals of ^{577}VLAEVITAAVR^{587} of Akap-8 display a modest increase in function of time (Fig. 3*C*), and as such the observed MS-pattern still falls within the statistically delineated region of efficient hGrB cleavage sites (Fig. 2). As for Bid, no proteolytic Akap-8 fragments could be observed by immunoblot analysis, though efficient cleavage was confirmed by the complete absence of the precursor substrate as early as 30 min following the addition of 10 nM of hGrB (Fig. 3*C* and Fig. 4). Processing of importin α-4 was found to lie outside the region of efficient cleavage events (Fig. 2) and was indeed confirmed as being the result of a far less efficiently cleaved hGrB site (only 48% of cleavage was detected following 2 h of incubation with 10 nM hGrB (Fig. 4)) as deduced from the gradual increase of the 50 kDa protein fragment generated upon ICED^{59} cleavage at later time-points (Fig. 3*D*). Finally, the three different nucleolin neo-N-termini identified, displayed large differences in the MS-signal intensities upon prolonged hGrB incubation (here shown in Fig. 3*E* for the neo-N terminus ^{476}TTEETLKESFDGSVR^{490}). Although all three identified cleavage events were predicted to be quite inefficient, the combined action of hGrB on all cleavage sites still resulted in a significant reduction of the precursor protein when challenged with hGrB, nevertheless nucleolin was found to be a far less efficiently cleaved substrate as compared with Bid, Bnip2 and Akap-8. The presence of a cleavage fragment

TABLE I

Categorization of 101 hGrB-generated neo-N-termini and their corresponding substrates. The UniProt database primary accession number, protein description, P10-P10' sequence and fold change of the neo-N-termini between 10 and 30 min and between 30 and 60 min are given. For each category, proteins are ranked alphabetically according to their protein description

SwissProt accession	Protein description	Human cleavage site P10-P10′	Fold change 10–30 min	Fold change 30–60 min
Efficient hGrB sites				
P63220	40S ribosomal protein S21	$MQND_{(4)}$ ↓ AGEFVDLYVP	0.89	1.33
O43823	A-kinase anchor protein 8	$KETPEEVAAD_{(576)}$ ↓ VLAEVITAAV	1.31	1.12
Q14562	ATP-dependent RNA helicase DHX8	$DEDDVKVAVD_{(144)}$ ↓ VLKELEALMP	0.98	1.03
Q12982	BCL2/adenovirus E1B 19 kDa protein-interacting protein 2	$LPEDDSIEAD_{(28)}$ ↓ ILAITGPEDQ	0.97	1.00
P55957	BH3-interacting domain death agonist	$HSRLGRIEAD_{(75)}$ ↓ SESQEDIIRN	1.30	1.06
Q9NUL3	Double-stranded RNA-binding protein Staufen homolog 2	$PKGILHLSPD_{(418)}$ ↓ VYQEMEASRH	1.03	1.02
P29083	General transcription factor IIE subunit 1	$MADPD_{(5)}$ ↓ VLTEVPAALK	1.21	1.24
Q6PKG0	La-related protein 1	$KDQDEQEELD_{(606)}$ ↓ FLFDEEMEQM	1.19	1.09
P18615	Negative elongation factor E	$SDRLRELGPD_{(149)}$ ↓ GEEAEGPGAG	0.86	1.29
P26599	Polypyrimidine tract-binding protein 1	$MDGIVPD_{(7)}$ ↓ IAVGTKRGSD	1.22	1.16
Q92733	Proline-rich protein PRCC	$LVPPQEIAPD_{(385)}$ ↓ ASFIDDEAFK	1.00	0.72
Q92974	Rho/Rac guanine nucleotide exchange factor 2	$REPALPLEPD_{(689)}$ ↓ SGGNTSPGVT	1.06	0.97
O75533	Splicing factor 3B subunit 1	$LDEAQGVGLD_{(34)}$ ↓ STGYYDQEIY	0.95	1.27
Q9Y2W1	Thyroid hormone receptor-associated protein 3	$REAQVNVRMD_{(574)}$ ↓ SFDEDLARPS	1.20	1.13
Q9Y5J1	U3 small nucleolar RNA-associated protein 18 homolog	$RCLEELVFGD_{(98)}$ ↓ VENDEDALLR	1.22	0.84
O43395	U4/U6 small nuclear ribonucleoprotein Prp3	$KRELKEVFGD_{(97)}$ ↓ DSEISKESSG	0.91	1.02
O95365	Zinc finger and BTB domain-containing protein 7A	$QILAADAGAD_{(139)}$ ↓ AGQLDLVDQI	1.15	1.10
Q6NZY4	Zinc finger CCHC domain-containing protein 8	$RTASGAVDED_{(513)}$ ↓ ALTLEELEEQ	1.16	1.20
Less efficient hGrB sites				
P62280	40S ribosomal protein S11	$QNKKRVLLGE_{(27)}$ ↓ TGKEKLPRYY	1.45	2.45
P62841	40S ribosomal protein S15	$KFTYRGVDLD_{(23)}$ ↓ QLLDMSYEQL	1.17	0.67
		$RGVDLDQLLD_{(27)}$ ↓ MSYEQLMQLY	1.31	1.67
		$LDQLLDMSYE_{(31)}$ ↓ QLMQLYSARQ	1.60	2.00
P62244	40S ribosomal protein S15a	$MVRMNVLAD_{(9)}$ ↓ ALKSINNAEK	2.25	1.47
P61247	40S ribosomal protein S3a	$GRVFEVSLAD_{(73)}$ ↓ LQNDEVAFRK	1.26	1.64
P62701	40S ribosomal protein S4, X isoform	$VAAPKHWMLD_{(21)}$ ↓ KLTGVFAPRP	1.17	2.08
		$RFAVHRITPE_{(117)}$ ↓ EAKYKLCKVR	2.00	2.53
P62081	40S ribosomal protein S7	$RSRTLTAVHD_{(127)}$ ↓ AILEDLVFPS	1.64	1.51
P10809	60 kDa heat shock protein, mitochondrial precursor	$RKPLVIIAED_{(277)}$ ↓ VDGEALSTLV	1.96	2.49
P27635	60S ribosomal protein L10	$FPLCGHMVSD_{(55)}$ ↓ EYEQLSSEAL	1.46	1.19
		$KWGFTKFNAD_{(179)}$ ↓ EFEDMVAEKR	1.08	1.71
P26373	60S ribosomal protein L13	$RKPSAPKKGD_{(138)}$ ↓ SSAEELKLAT	1.51	1.78
P84098	60S ribosomal protein L19	$GKKKVWLDPN_{(27)}$ ↓ ETNEIANANS	1.23	2.18
P61254	60S ribosomal protein L26	$NVRSMPIRKD_{(52)}$ ↓ DEVQVVRGHY	1.41	3.40
P39023	60S ribosomal protein L3	$VPVNQVFGQD_{(214)}$ ↓ EMIDVIGVTK	1.66	1.27
P46777	60S ribosomal protein L5	$YEGQVEVTGD_{(128)}$ ↓ EYNVESIDGQ	1.41	1.99
Q01813	6-phosphofructokinase type C	$NMGGLAAGAD_{(601)}$ ↓ AAYIFEEPFD	1.78	2.65
P17858	6-phosphofructokinase, liver type	$PGTDFSLGSD_{(542)}$ ↓ TAVNAAMESC	2.45	2.35
P08237	6-phosphofructokinase, muscle type	$PGSDFSVGAD_{(543)}$ ↓ TALNTICTTC	1.55	1.76
P60709	Actin, cytoplasmic 1	$KEKLCYVALD_{(222)}$ ↓ FEQEMATAAS	1.22	8.26
Q9UG63	ATP-binding cassette sub-family F member 2	$ANGRETTEVD_{(54)}$ ↓ LLTKELEDFE	2.27	1.17
Q92499	ATP-dependent RNA helicase DDX1	$NCTISQVEPD_{(676)}$ ↓ IKVPVDEFDG	0.98	1.79
P55210	Caspase-7 precursor	$TELDDGIQAD_{(198)}$ ↓ SGPINDTDAN	1.35	0.77
Q99459	Cell division cycle 5-like protein	$PARPDPIDMD_{(145)}$ ↓ EDELEMLSEA	1.13	1.94
Q14839	Chromodomain-helicase-DNA-binding protein 4	$EDDDLDVESD_{(320)}$ ↓ FDDASINSYS	1.45	1.28
O00273	DNA fragmentation factor subunit alpha	$MEVTGD_{(6)}$ ↓ AGVPESGEIR	1.92	2.42
P49736	DNA replication licensing factor MCM2	$RDYRAIPELD_{(88)}$ ↓ AYEAEGLALD	1.98	2.09
P33992	DNA replication licensing factor MCM5	$FDDPGIFYSD_{(13)}$ ↓ SFGGDAQADE	1.74	1.92
P68104	Elongation factor 1-alpha 1	$DGPKFLKSGD_{(398)}$ ↓ AAIVDMVPGK	1.47	2.60
		$MVPGKPMCVE_{(413)}$ ↓ SFSDYPPLGR	1.32	2.41
Q04637	Eukaryotic translation initiation factor 4 gamma 1	$RLQGINCGPD_{(665)}$ ↓ FTPSFANLGR	1.19	1.52
Q92945	Far upstream element-binding protein 2	$RQIAAKIGGD_{(91)}$ ↓ AATTVNNSTP	1.08	2.03
P85037	Forkhead box protein K1	$SGGSSGVSGD_{(80)}$ ↓ SAVAGAAPAL	1.34	1.04
P14314	Glucosidase 2 subunit beta precursor	$AEAQALLSGD_{(260)}$ ↓ TQTDATSFYD	1.22	1.76
Q14527	Helicase-like transcription factor	$IPPDDFLTSD_{(52)}$ ↓ EEVDSVLFGS	1.71	1.67
P61978	Heterogeneous nuclear ribonucleoprotein K	$GEFGKRPAED_{(26)}$ ↓ MEEEQAFKRS	1.42	1.53
Q00839	Heterogeneous nuclear ribonucleoprotein U	$VAGFKKQMAD_{(547)}$ ↓ TGKLNTLLQR	1.67	3.65
P0C0S5	Histone H2A.Z	$MAGGKAGKD_{(9)}$ ↓ SGKAKTKAVS	5.77	1.14
O00629	Importin subunit alpha-4	$NVPHEDICED_{(59)}$ ↓ SDIDGDYRVQ	1.33	1.21
Q12906	Interleukin enhancer-binding factor 3	$LFPDTPLALD_{(597)}$ ↓ ANKKKRAPVP	1.27	2.44

TABLE I—*continued*

SwissProt accession	Protein description	Human cleavage site P10-P10′	Fold change 10–30 min	Fold change 30–60 min
Q32MZ4	Leucine-rich repeat flightless-interacting protein 1	AAEEVLADGD$_{(675)}$ ↓ TLDFEDDTVQ	1.49	2.11
O60711	Leupaxin	MEELD$_{(5)}$ ↓ ALLEELERST	1.70	2.77
Q15046	Lysyl-tRNA synthetase	HTTDNGVGPE$_{(67)}$ ↓ EESVDPNQYY	1.49	2.40
P56192	Methionyl-tRNA synthetase, cytoplasmic	TPQQTKITQD$_{(368)}$ ↓ IFQQLLKRGF	2.36	2.25
P27816	Microtubule-associated protein 4	KKCSLPAEED$_{(642)}$ ↓ SVLEKLGERK	1.57	2.23
Q9BQG0	Myb-binding protein 1A	LGDEAMMALD$_{(790)}$ ↓ QSLASLFAEQ	1.49	2.09
P67809	Nuclease-sensitive element-binding protein 1	QYSNPPVQGE$_{(216)}$ ↓ VMEGADNQGA	1.55	1.88
Q9NR30	Nucleolar RNA helicase 2	MPGKLRSD$_{(8)}$ ↓ AGLESDTAMK	1.03	1.65
P19338	Nucleolin	KNLPYKVTQD$_{(407)}$ ↓ ELKEVFEDAA	1.52	1.29
		AYIEFKTEAD$_{(441)}$ ↓ AEKTFEEKQG	2.06	1.74
		TLFVKGLSED$_{(582)}$ ↓ TTEETLKESF	2.20	2.09
P55209	Nucleosome assembly protein 1-like 1	NKEQSELDQD$_{(15)}$ ↓ LDDVEEVEEE	2.07	1.88
O75475	PC4 and SFRS1-interacting protein	KNMFLVGEGD$_{(433)}$ ↓ SVITQVLNKS	1.37	2.08
Q8WUA2	Peptidyl-prolyl cis-trans isomerase-like 4	QLDSGRIGAD$_{(194)}$ ↓ EEIDDFKGRS	1.43	1.62
O60828	Polyglutamine-binding protein 1	PEPEEEIIAE$_{(31)}$ ↓ DYDDDPVDYE	1.41	1.83
P26599	Polypyrimidine tract-binding protein 1	ALAASAAAVD$_{(172)}$ ↓ AGMAMAGQSP	1.17	1.47
Q96GQ7	Probable ATP-dependent RNA helicase DDX27	ADENILTKAD$_{(187)}$ ↓ TLKVKDRKKK	1.06	0.54
Q9UQ80	Proliferation-associated protein 2G4	RITSGPFEPD$_{(341)}$ ↓ LYKSEMEVQD	2.19	2.52
Q8N163	Protein KIAA1967	ETEPTEQAPD$_{(469)}$ ↓ ALEQAADTSR	1.20	2.00
O15355	Protein phosphatase 1G	DNEEAALLHE$_{(147)}$ ↓ EATMTIEELL	1.67	2.38
		MEGKEEPGSD$_{(326)}$ ↓ SGTTAVVALI	2.24	3.42
P06454	Prothymosin alpha [Contains: Thymosin alpha-1]	MSDAAVD$_{(7)}$ ↓ TSSEITTKDL	2.13	2.48
P06400	Retinoblastoma-associated protein	PPPEEDPEQD$_{(36)}$ ↓ SGPEDLPLVR	1.84	1.83
Q9H814	RNA U small nuclear RNA export adapter protein	EQNQDAVATE$_{(133)}$ ↓ LGILGMEGTI	1.80	2.39
P98175	RNA-binding protein 10	DERRESATAD$_{(691)}$ ↓ AGYAILEKKG	1.21	1.65
O75533	Splicing factor 3B subunit 1	YFDKLLVDVD$_{(483)}$ ↓ ESTLSPEEQK	1.53	1.42
Q13435	Splicing factor 3B subunit 2	TKPKLTIHGD$_{(566)}$ ↓ LYYEGKEFET	1.39	2.03
		DETGFITPAD$_{(719)}$ ↓ SGLITPGGFS	1.53	3.04
Q86YP4	Transcriptional repressor p66-alpha	KSERRPPSPD$_{(102)}$ ↓ VIVLSDNEQP	2.50	2.58
Q71U36	Tubulin alpha-1A chain	KHVPRAVFVD$_{(69)}$ ↓ LEPTVIDEVR	0.90	3.54
		GTYRQLFHPE$_{(90)}$ ↓ QLITGKEDAA	2.31	2.38
		LRFDGALNVD$_{(251)}$ ↓ LTEFQTNLVP	1.68	2.48
P07437	Tubulin beta chain	IDPTGTYHGD$_{(39)}$ ↓ SDLQLDRISV	2.71	2.45
Q14694	Ubiquitin carboxyl-terminal hydrolase 10	EYQRIEFGVD$_{(62)}$ ↓ EVIEPSDTLP	1.00	1.98
Q9NZ63	Uncharacterized protein C9orf78	QMLSGIPEVD$_{(177)}$ ↓ LGIDAKIKNI	1.88	2.40
P53990	Uncharacterized protein KIAA0174	AEAPPGVETD$_{(194)}$ ↓ LIDVGFTDDV	1.04	2.24
P54725	UV excision repair protein RAD23 homolog A	LADISDVEGE$_{(300)}$ ↓ VGAIGEEAPQ	1.80	2.25
P46459	Vesicle-fusing ATPase	IKASTKVEVD$_{(466)}$ ↓ MEKAESLQVT	2.10	1.88
P08670	Vimentin	QDSVDFSLAD$_{(90)}$ ↓ AINTEFKNTR	1.23	2.66
		QIQEQHVQID$_{(257)}$ ↓ VDVSKPDLTA	1.07	2.05
		QEQHVQIDVD$_{(259)}$ ↓ VSKPDLTAAL	1.51	2.16
Q9UHR6	Zinc finger HIT domain-containing protein 2	EELDNAPGSD$_{(150)}$ ↓ AAELELAPAR	2.22	1.13

close to the precursor band on Western blot occluded straightforward densitometric analysis, implying that the degree of cleavage could not be determined.

Validation of Cleavage Events using Peptide Mimetics—For some substrates the sizes of the generated proteolytic fragments observed on Western blot were not in accordance with the expected theoretical molecular weights based on the identified cleavage sites. Together with the presence of additional fragments for some of these substrates, this precluded unambiguous assignment and validation of hGrB cleavage efficiency as observed for single proteolytic events (*e.g.* Fig. 3*E*). Therefore, the degree of cleavage of peptide substrates holding the identified cleavage site was determined in a RP-HPLC assay. For the synthetic peptides holding the identified cleavage sites of Bid, Bnip-2, and Akap-8, complete cleavage was observed following incubation with 500 nM of hGrB for 2 h (Supplemental Figs. 2*A–C*), agreeing with our proteomics data and immunoblot analysis. The peptide holding the hGrB site of importin α-4 was here also found to be less efficiently processed (*i.e.* 59% processed at 500 nM of hGrB, Supplemental Fig. 2*D*), again agreeing with our proteomics and immunoblot data. For some other peptide substrates of which the proteomics analysis yielded fold-changes deviating significantly from those of protein N-termini, hGrB cleavage was not observed or only found to occur less than 5% even at the highest concentration of hGrB (examples are protein phosphatase 1G, nucleolin and microtubule-associated protein 4 (data not shown and Supplemental Fig. 2*E*)), verifying these as inefficiently cleaved hGrB sites. Overall, the degree of peptide cleavage followed the degree of protein processing and concomitantly validated the results from the proteomics screen.

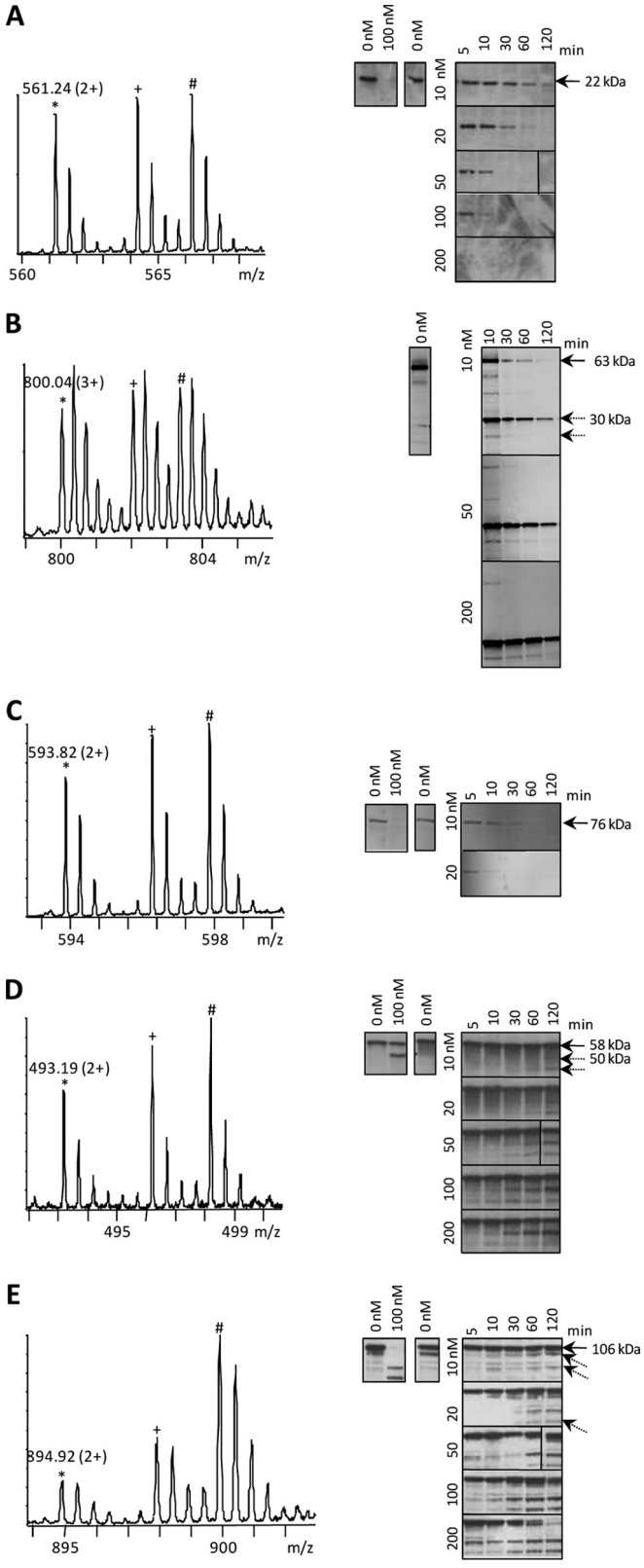

FIG. 3. **Biochemical characterization of the categorized efficiency of cleavage of the hGrB substrates Bid, Bnip2, Akap-8 (all categorized as "efficiently cleaved"), importin α-4, and nucleolin (categorized as "less efficiently cleaved").** The peptide ion triplets shown in the MS-spectra represent hGrB-specific neo-N-terminal peptides identified in Jurkat freeze-thaw lysates treated with human recombinant GrB for 10 ($^{12}C_6$, *, m/z value and charge indicated), 30 ($^{13}C_6$, +) or 60 ($^{13}C_6{}^{15}N_4$, #) minutes. The corresponding peptides were AcD3-^{76}SESQEDIIR^{84} from Bid (*A*), AcD3-^{29}ILAITGPEDQPGSLEVNGNKVR^{50} from Bnip2 (*B*), AcD3-^{577}VLAEVITAAVR^{587} from Akap-8 (*C*), AcD3-^{60}SDIDGDYR^{67} from the importin subunit alpha-4 (*D*), and AcD3-^{476}TTEETLKESFDGSVR^{490} from nucleolin (*E*). GrB-mediated processing of the corresponding substrates was assayed by Western blotting using antibodies directed against these substrates (see also Methods section). In each panel, Western blots shown at the right side are from cell lysates that were pre-incubated with iodoacetamide and treated with different concentrations of hGrB for various incubation periods. When the molecular weights of protein fragments (indicated with striped arrows) agreed with the fragment sizes as determined by the degradomics screen, the molecular weight values are indicated. Western blots shown at the left side are from control cell lysates that were non pre-incubated with iodoacetamide.

DISCUSSION

In this study, a gel-free method, combining metabolic labeling with N-terminal COFRADIC was used to study quantitative aspects of substrate proteolysis by human granzyme B. Time-based concentration fluxes of previously assigned hGrB-specific neo-N-termini (1) were assayed against the distribution of database-annotated, hGrB unaffected protein N-termini. 101 hGrB-specific neo-N-termini from 86 human Jurkat proteins were categorized according to their cleavage efficiency. Our assay assigned the pro-apoptotic Bcl-2 family member Bid, which lies at a pivotal point in hGrB-induced apoptosis, as possessing one of hGrB's most efficient sites. This illustrates that our approach is capable of revealing a critical substrate cleavage event implicated in protease-mediated signaling. In this respect, the pro-apoptotic Bcl-2 family member Bnip2 and Akap-8, both of which are known to play prominent roles in apoptotic execution (20, 21), are here also identified as holding efficiently cleaved hGrB specific sites.

In a model of natural killer cytotoxic granule-mediated K-562 cell death, 14 hGrB-specific physiological cleavage sites were identified (1). Interestingly, in our current study six of these sites were identified and three—processing of Bid, Akap-8, and the zinc finger CCHC domain-containing protein 8—were categorized as efficient hGrB cleavage events. These results again hint to possible physiological more important cleavage sites. One could argue that similar kinetics studies could be applied to monitor substrate processing in such physiological more relevant cellular setups however, an increased variability of perforin-mediated delivery, in case of granzyme B, next to an overall reduced kinetics of proteolysis and possible decrease in the stability of generated proteolytic fragments in intact cells would make the assignment of critical cleavage events more troublesome in cellular systems.

Of note is that the observed efficiency for individual cleavage events cannot be directly extrapolated to the substrate level. By itself, the turnover of the precursor substrate reflects

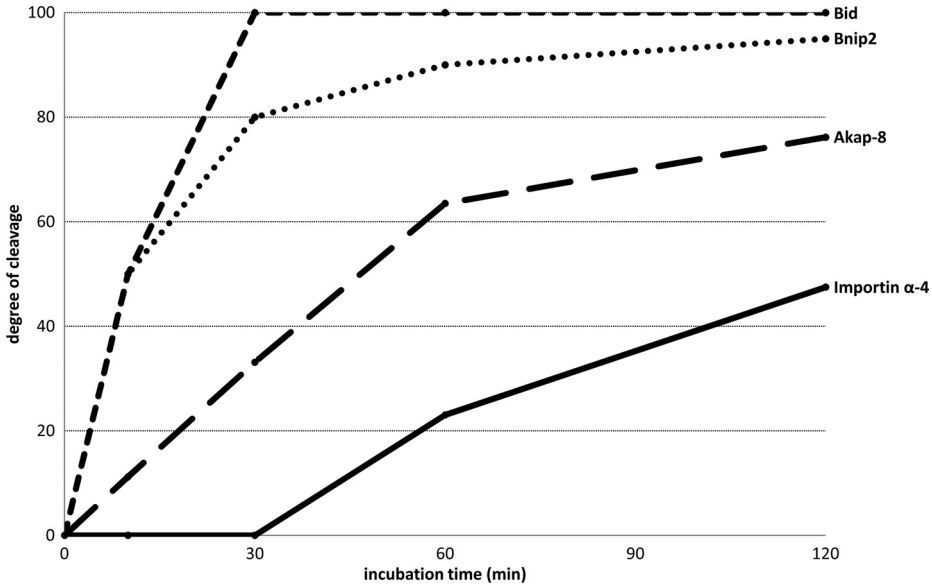

FIG. 4. **Degrees of hGrB processing at various time points determined for Bid, Bnip2, Akap-8, and importin α-4.** Percentages of substrate cleavage were determined by densitometry following Western blot analyses using 10 nM of hGrB for 10, 30, 60, and 120 min. MS/MS spectra of all categorized hGrB neo-N-termini are available in PDF format. The highest scoring spectra (n=101) and corresponding lower scoring spectra (n = 130) are available in the PDF-files: "MS-MS_highest_scoring_spectra" and "MS-MS_lower_scoring_spectra" respectively.

the total efficiency by which the substrate is cleaved at different sites as observed for nucleolin (Fig. 3*E*). On the other hand, the identification of one efficient cleavage event suffices to consider the substrate as an efficiently cleaved one. The opposite however, the identification of a rather inefficient cleavage event reflecting a poorly cleaved substrate, does not necessarily hold true.

Another shortcoming of our approach is exemplified by the identification of three neighboring hGrB cleavage sites in the 40S ribosomal protein S15 (VDLD$^{24}\downarrow$QLLD$^{28}\downarrow$MSYE$^{32}\downarrow$QLMQLYSAR^{40}, Supplemental Fig. 3). This is a situation in which neo-N-termini are identified that hold additional, nested hGrB cleavage sites. As a consequence the fold change observed in MS spectra for neo-N-terminal peptides holding such indirect cleavage sites might therefore lead to an erroneous categorization of such cleavages. In the same respect, although caspase-7 did not make it to the list of efficient substrates, Western blot analyses performed by Adrain *et al.* demonstrated that Bid and caspase-7 were cleaved by hGrB with equal efficiencies, and further revealed that caspase-7 was cleaved at least at two different sites (24). As such, caspase-7 probably would have made it on our list of efficiently cleaved substrates, but because of a secondary cleavage event, extrapolation of caspase-7 cleavage efficiency from the MS-spectrum resulting from the primary cleavage, is compromised. This observation further hints that substrate processing efficiencies of promiscuous proteases will be much more challenging to assay by our approach.

The apparent acceleration of cleavage at inefficient granzyme B recognition sites (Fig. 2), which does not follow the expected standard first order kinetics, was unanticipated. We reasoned that in complex mixtures such as the proteome assayed in this study, efficient substrates are initially consumed by granzyme B, after which granzyme B is "liberated" and starts to increasingly process inefficient sites. We tested our hypothesis by assaying granzyme B processing of the fluorogenic peptide Ac-IEPD-AMC, both in granzyme B buffer as well as in a Jurkat cell lysate using similar concentrations of granzyme B and proteome as used in our proteomics study. Ac-IEPD-AMC has a reported K_m value of 370 μM $\pm$ 70 μM—note that we here measured a K_m value of 461 μM $\pm$ 26 μM—and is thus an inefficient substrate, with low affinity for granzyme B (25). Overall, the absence of first-order cleavage of Ac-IEPD-AMC, deduced from the acceleration of cleavage observed at earlier time-points when the peptide was assayed in the cell lysate (Supplemental Fig. 4), corresponds with our observations in the proteomics setup (Fig. 2) and thus confirms that processing at inefficient sites in full proteomes is accelerated once efficient sites are processed.

Selected reaction monitoring (SRM) appears to be an attractive and alternative MS-based method to probe the extent of proteolysis. SRM allows quantification of peptides by targeting a predetermined set peptide-to-fragment transitions (26). When combined with spiked-in internal standard peptides, SRM allows for the specific (absolute) quantification of a modest to high number of peptides present in rather complex peptide mixtures. As for degradomics studies however, prior knowledge of cleavage events is mandatory and as such SRM may be more suited to study selected and already characterized proteolytic events in several cellular setups.

Overall, and because cell-free reconstruction of biochemical relevant proteolytic pathways have proven to be representative in a cellular context (24), we here show that our multiplexed degradomics screen by probing the efficiency of protease cleavage events might be an interesting asset to map the segment of critical protease substrates.

Acknowledgment—We would like to thank Niklaas Colaert for bioinformatics assistance.

* K.P. and K.H. are supported by Ph.D grants from the institute for the Promotion of Innovation through Science and Technology in Flanders (IWT-Vlaanderen). P.V.D. and F.I. are Postdoctoral Fellows of the Research Foundation - Flanders (FWO-Vlaanderen). We further acknowledge support of research grants from the Fund for Scientific Research - Flanders (Belgium) (project numbers G.0077.06 and G.0042.07), the Concerted Research Actions (project BOF07/GOA/012) from the Ghent University and the Inter University Attraction Poles (IUAP06).

S This article contains supplemental Figs. 1–4 and Table 1.

† Both authors contributed equally to this work.

‖ To whom all correspondence should be addressed: Department of Medical Protein Research, Flanders Interuniversity Institute for Biotechnology, Ghent University, A. Baertsoenkaai 3, B9000 Ghent, Belgium. Tel.: +32-92649274; Fax: +32-92649496; E-mail: kris.gevaert@vib-ugent.be or petra.vandamme@vib-ugent.be.

REFERENCES

1. Van Damme, P., Maurer-Stroh, S., Plasman, K., Van Durme, J., Colaert, N., Timmerman, E., De Bock, P. J., Goethals, M., Rousseau, F., Schymkowitz, J., Vandekerckhove, J., and Gevaert, K. (2009) Analysis of protein processing by N-terminal proteomics reveals novel species-specific substrate determinants of granzyme B orthologs. *Mol. Cell Proteomics* **8,** 258–272
2. Trapani, J. A., and Smyth, M. J. (2002) Functional significance of the perforin/granzyme cell death pathway. *Nat. Rev. Immunol.* **2,** 735–747
3. Romero, V., and Andrade, F. (2008) Non-apoptotic functions of granzymes. *Tissue Antigens* **71,** 409–416
4. Impens, F., Colaert, N., Helsens, K., Plasman, K., Van Damme, P., Vandekerckhove, J., and Gevaert, K. (2010) MS-driven protease substrate degradomics. *Proteomics* **10,** 1284–1296
5. Enoksson, M., Li, J., Ivancic, M. M., Timmer, J. C., Wildfang, E., Eroshkin, A., Salvesen, G. S., and Tao, W. A. (2007) Identification of Proteolytic Cleavage Sites by Quantitative Proteomics. *J. Proteome Res.* **6,** 2850–2858
6. Timmer, J. C., and Salvesen, G. S. (2007) Caspase substrates. *Cell Death Differ.* **14,** 66–72
7. Staes, A., Van Damme, P., Helsens, K., Demol, H., Vandekerckhove, J., and Gevaert, K. (2008) Improved recovery of proteome-informative, protein N-terminal peptides by combined fractional diagonal chromatography (COFRADIC). *Proteomics* **8,** 1362–1370
8. Gevaert, K., Goethals, M., Martens, L., Van Damme, J., Staes, A., Thomas, G. R., and Vandekerckhove, J. (2003) Exploring proteomes and analyzing protein processing by mass spectrometric identification of sorted N-terminal peptides. *Nat. Biotechnol.* **21,** 566–569
9. Ong, S. E., Blagoev, B., Kratchmarova, I., Kristensen, D. B., Steen, H., Pandey, A., and Mann, M. (2002) Stable isotope labeling by amino acids in cell culture, SILAC, as a simple and accurate approach to expression proteomics. *Mol. Cell Proteomics* **1,** 376–386
10. Sun, J., Bird, C. H., Thia, K. Y., Matthews, A. Y., Trapani, J. A., and Bird, P. I. (2004) Granzyme B encoded by the commonly occurring human RAH allele retains pro-apoptotic activity. *J. Biol. Chem.* **279,** 16907–16911
11. Sun, J., Bird, C. H., Buzza, M. S., McKee, K. E., Whisstock, J. C., and Bird, P. I. (1999) Expression and purification of recombinant human granzyme B from Pichia pastoris. *Biochem. Biophys. Res. Commun.* **261,** 251–255
12. Ghesquière, B., Van, Damme, J., Martens, L., Vandekerckhove, J., and Gevaert, K. (2006) Proteome-wide characterization of N-glycosylation events by diagonal chromatography. *J. Proteome Res.* **5,** 2438–2447
13. Martens, L., Vandekerckhove, J., and Gevaert, K. (2005) DBToolkit: processing protein databases for peptide-centric proteomics. *Bioinformatics* **21,** 3584–3585
14. Van Damme, P., Martens, L., Van Damme, J., Hugelier, K., Staes, A., Vandekerckhove, J., and Gevaert, K. (2005) Caspase-specific and non-specific in vivo protein processing during Fas-induced apoptosis. *Nat. Methods* **2,** 771–777
15. Huber, P. J., Ronchetti, E.M. (2009) *Robust Statistics*, 2nd Ed., Wiley, John and Sons
16. Demon, D., Van Damme, P., Vanden Berghe, T., Deceuninck, A., Van Durme, J., Verspurten, J., Helsens, K., Impens, F., Wejda, M., Schymkowitz, J., Rousseau, F., Madder, A., Vandekerckhove, J., Declercq, W., Gevaert, K., and Vandenabeele, P. (2009) Proteome-wide substrate analysis indicates substrate exclusion as a mechanism to generate caspase-7 versus caspase-3 specificity. *Mol. Cell Proteomics* **8,** 2700–2714
17. Casciola-Rosen, L., Garcia-Calvo, M., Bull, H. G., Becker, J. W., Hines, T., Thornberry, N. A., and Rosen, A. (2007) Mouse and human granzyme B have distinct tetrapeptide specificities and abilities to recruit the bid pathway. *J. Biol. Chem.* **282,** 4545–4552
18. Andrade, F., Roy, S., Nicholson, D., Thornberry, N., Rosen, A., and Casciola-Rosen, L. (1998) Granzyme B directly and efficiently cleaves several downstream caspase substrates: implications for CTL-induced apoptosis. *Immunity* **8,** 451–460
19. Trapani, J. A., and Sutton, V. R. (2003) Granzyme B: pro-apoptotic, antiviral and antitumor functions. *Curr. Opin. Immunol.* **15,** 533–543
20. Valencia, C. A., Cotten, S. W., and Liu, R. (2007) Cleavage of BNIP-2 and BNIP-XL by caspases. *Biochem. Biophys. Res. Commun.* **364,** 495–501
21. Kamada, S., Kikkawa, U., Tsujimoto, Y., and Hunter, T. (2005) A-kinase-anchoring protein 95 functions as a potential carrier for the nuclear translocation of active caspase 3 through an enzyme-substrate-like association. *Mol. Cell. Biol.* **25,** 9469–9477
22. Thornberry, N. A., Rano, T. A., Peterson, E. P., Rasper, D. M., Timkey, T., Garcia-Calvo, M., Houtzager, V. M., Nordstrom, P. A., Roy, S., Vaillancourt, J. P., Chapman, K. T., and Nicholson, D. W. (1997) A combinatorial approach defines specificities of members of the caspase family and granzyme B. Functional relationships established for key mediators of apoptosis. *J. Biol. Chem.* **272,** 17907–17911
23. Barry, M., Heibein, J. A., Pinkoski, M. J., Lee, S. F., Moyer, R. W., Green, D. R., and Bleackley, R. C. (2000) Granzyme B short-circuits the need for caspase 8 activity during granule-mediated cytotoxic T-lymphocyte killing by directly cleaving Bid. *Mol. Cell. Biol.* **20,** 3781–3794
24. Adrain, C., Murphy, B. M., and Martin, S. J. (2005) Molecular ordering of the caspase activation cascade initiated by the cytotoxic T lymphocyte/natural killer (CTL/NK) protease granzyme B. *J. Biol. Chem.* **280,** 4663–4673
25. Ruggles, S. W., Fletterick, R. J., and Craik, C. S. (2004) Characterization of structural determinants of granzyme B reveals potent mediators of extended substrate specificity. *J. Biol. Chem.* **279,** 30751–30759
26. Lange, V., Picotti, P., Domon, B., and Aebersold, R. (2008) Selected reaction monitoring for quantitative proteomics: a tutorial. *Mol. Syst. Biol.* **4,** 222
27. Scott, G. B., Bowles, P. A., Wilson, E. B., Meade, J. L., Low, B. C., Davison, A., Blair, G. E., and Cook, G. P. (2010) Identification of the BCL2/adenovirus E1B-19K protein-interacting protein 2 (BNIP-2) as a granzyme B target during human natural killer cell-mediated killing. *Biochem. J.* **431,** 423–431